# Probing the oxygen vacancy distribution in resistive switching Fe-$SrTiO_3$ metal-insulator-metal-structures by micro-x ray absorption near-edge structure

Ch. Lenser, A. Kuzmin, J. Purans, A. Kalinko, R. Waser, and R. Dittmann

Citation: Journal of Applied Physics **111**, 076101 (2012);
View online: https://doi.org/10.1063/1.3699315
View Table of Contents: http://aip.scitation.org/toc/jap/111/7
Published by the American Institute of Physics



# Probing the oxygen vacancy distribution in resistive switching Fe-$SrTiO_3$ metal-insulator-metal-structures by micro-x ray absorption near-edge structure

Ch. Lenser,[1,2,a)] A. Kuzmin,[3] J. Purans,[3] A. Kalinko,[3] R. Waser,[1,2,4] and R. Dittmann[1,2]
[1]*Peter Grünberg Institut, Forschungszentrum Jülich, Jülich 52425, Germany*
[2]*Jülich-Aachen Research Alliance, Section Fundamentals of Future Information Technology (JARA-FIT), Germany*
[3]*Institute of Solid State Physics, University of Latvia, Kengaraga Street 8, Riga LV-1063, Latvia*
[4]*Institut für Werkstoffe der Elektrotechnik, RWTH Aachen, Aachen 52056, Germany*

(Received 2 March 2012; accepted 4 March 2012; published online 4 April 2012)

Resistive switching metal-insulator-metal structures were fabricated from epitaxial Fe-doped $SrTiO_3$ thin films to study the distribution of oxygen vacancies in a switched memristor cell using a micro-focused x-ray beam. In addition to the main filament, we found that the concentration of oxygen vacancies increases homogeneously over the whole electrode area during the electroforming procedure. The x-ray absorption near-edge structure (XANES) observed at the location of the filament exhibits distinct differences to the surrounding area, which are interpreted with full-multiple-scattering XANES calculations to derive from oxygen vacancy clustering in the first coordination shell around Fe. © *2012 American Institute of Physics*. [http://dx.doi.org/10.1063/1.3699315]

Binary and ternary metal oxides as emergent materials for non-volatile memory applications are receiving an increasing amount of scientific attention, due to the promising scalability, retention, and switching characteristics of this material class.[1,2] The key role of oxygen non-stoichiometry and oxygen-deficient oxide-phases as the underlying mechanism of the resistance change has been recognized for many different oxide systems (e.g., $TiO_2$,[3,4] $Ta_2O_5$,[5] $SrTiO_3$.[6] It is becoming widely accepted that the resistance switching process in $SrTiO_3$ is related to the movement of oxygen vacancies and the associated electron doping. The mechanism of electroforming in Pt/Fe:$SrTiO_3$/Nb:$SrTiO_3$ metal-insulator-metal (MIM) structures suggested by Menke *et al.*[6] proposes the local bypassing of the interfacial Schottky-type barrier by oxygen-deficient filaments forming along extended defects. It is assumed that the films are already oxygen deficient after deposition. While this model is well supported by the electrical behavior of the devices, direct experimental observation of the oxygen deficiency and the formation of the conducting filament has so far been reported for a few polycrystalline, binary oxides,[7] but not for single crystalline thin films of complex oxides. The presence of oxygen vacancies in the first coordination shell of transition-metal (TM) dopants can be traced by x-ray absorption near-edge structure (XANES) through a characteristic increase of intensity in the pre-edge region of the TM K-edge.[8,9] This approach was used to interpret the spatial distribution of TM-$V_O^{\bullet\bullet}$ defect associates in the material, and extended channels of oxygen vacancies have been demonstrated by micro-XANES ($\mu$XANES) in Cr-doped $SrTiO_3$ single crystals.[8,10]

In this letter, we examine $\mu$m-sized thin-film memristor devices with $\mu$XANES and utilize the sensitivity of the TM K-edge to obtain information about the local changes around the TM-dopant induced by resistive switching and their spatial distribution in the MIM-structure. Since the absorption length of TM K$\alpha$ fluorescence is several $\mu$m in $SrTiO_3$, the $\mu$XANES experiment is bulk-sensitive and provides information about the whole film.

Memristive devices were fabricated from $SrTi_{0.95}Fe_{0.05}O_3$ thin films (thickness = 200 nm) grown by pulsed laser deposition (PLD) on a conducting Nb-doped $SrTiO_3$ single crystal (CrysTec GmbH, Berlin) at a substrate temperature of 700 °C and oxygen pressure of 0.25 mbar, using a KrF excimer laser ($\lambda = 248$ nm) and a laser fluence of 0.8 J/cm$^2$ at the target. A 30-nm Pt layer was sputtered onto the insulating layer and structured via UV-lithography and reactive ion beam etching (RIBE).

After the initially insulating devices are electroformed with a DC voltage of +7 V (voltage bias applied to the Pt top-electrode), the MIM structures are switching in a "counter-eightwise" polarity,[11] as depicted in Fig. 1. The low resistance "Set" state is reached by applying a negative bias to the top electrode, electrostatically attracting $V_O^{\bullet\bullet}$ to the Pt. A sufficiently high concentration will result in an ohmic current response to a small read-out voltage (Fig. 1(b)), whereas the current response of the memristor in the high resistance "Reset" state is distinctly non-linear. This state is reached by applying a positive bias to the top electrode, repulsing $V_O^{\bullet\bullet}$ and lowering the local charge carrier concentration.

Iron K-edge XANES experiments were performed at the ID03 beamline at the European Synchrotron Radiation Facility (ESRF) equipped with a monolithic channel-cut Si(111) monochromator and a Kirkpatrick-Baez (KB)-mirror focusing optics to obtain a beam diameter of 7 $\mu$m. The Fe K-edge XANES was measured in fluorescence mode by placing the sample and a silicon drift detector (SDD) perpendicular to the incoming x

a)Electronic mail: c.lenser@fz-juelich.de.

 

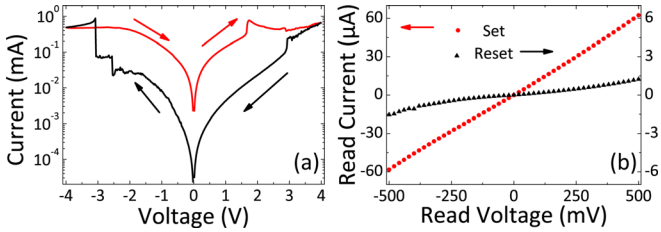


FIG. 1. (a) Current-voltage characteristics of the Pt/200 nm $SrTi_{0.95}Fe_{0.05}O_3$/Nb:STO memristor. The switching polarity is indicated by the arrows. (b) Current response to a low read-out voltage, highlighting the change of the conduction mechanism between "Set" and "Reset" state (red and black symbols, respectively).

ray beam (90° geometry). While the Fe Kα fluorescence derives from the thin film only, the Ti Kα fluorescence, which was measured simultaneously as a reference, has an escape depth of several μm and originates mainly from the substrate.

Iron acts as a B-site acceptor dopant in $SrTiO_3$ and can be used as a tracer to track the valence change and presence of oxygen vacancy associates in the material.[9] As a reference, we will use a Fe-doped $SrTiO_3$ single crystal that has been subjected to a long-term dc voltage at moderately elevated temperature. Such treatment induces an ion concentration polarization and a corresponding oxidation and reduction near the anode and cathode, respectively, which leads to pronounced coloration at the anode (called *electrocoloration*) because of the Fe doping. Figure 2 shows the Fe K-edge XANES of an as-deposited thin film compared with two spectra recorded at cathode and anode of the electrocolored single crystal that contains predominantly $Fe^{3+}$ with a significant amount of Fe-$V_O^{\bullet\bullet}$ (cathode), as well as one that contains mostly $Fe^{4+}$ and no Fe-$V_O^{\bullet\bullet}$ (anode; for details, see Ref. 9). The spectral difference visible at the strongly reduced cathode (see shoulder S) is caused by the presence of Fe-$V_O^{\bullet\bullet}$ complexes, and the resemblance of the XANES indicates a similar degree of association of Fe-$V_O^{\bullet\bullet}$ in the as-deposited film and the cathode. However, the MIM cells remain insulating ($R > 10^{11}\,\Omega$), because the charge carriers introduced by the oxygen vacancies are partially compensated by the high acceptor doping. Considering Fig. 2, it is obvious that the resistance change in the thin film does not rely on the $Fe^{3+}/Fe^{4+}$ redox pair, as the film does not contain $Fe^{4+}$.

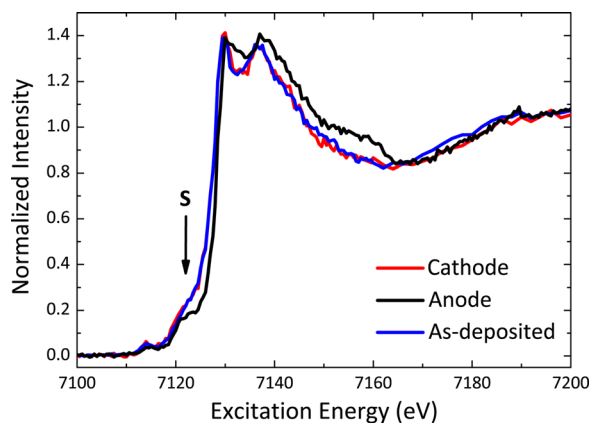


FIG. 2. Fe K-edge XANES of the as-deposited thin film (blue) as well as the cathode (red) and anode (black) regions of an electrocolored Fe-doped $SrTiO_3$ single crystal.

A micro-focused x-ray beam was used to record XY-maps (Fig. 3(a)) of the oxygen vacancy concentration on a MIM structure in the low-resistance "Set" state by measuring the Fe Kα fluorescence intensity at the excitation energy 7122 eV, i.e., at the maximum contrast in the pre-edge region caused by vacancies and indicated by the shoulder S (Fig. 3(b)). The XY-scanning was performed with a step size 2 μm and an x ray beam diameter of 7 μm. The mapping reveals a single location with a large fluorescence intensity increase compared to the surrounding electrode (see dashed, red box in Fig. 3(a)), which can be attributed to the location of the conducting filament. We note that, outside of the electrode area, the apparent increase of S is an artifact caused by a higher total fluorescene intensity, since the radiation is not attenuated by the electrode material. The Fe K-edge XANES measured at several locations on the electrode pad (Fig. 3(b), blue) and at the filament location (red) confirms that the intensity of S is increased homogeneously over the whole electrode area as compared to the as-deposited film (black). A non-resonant Ti Kα map recorded simultaneously shows the top electrode to be free of holes or structural artifacts that could lead to the observed Fe Kα intensity increase (data not shown here). The Fe K-edge XANES was also measured on a different electrode pad that had been subjected to an irreversible, "hard" dielectric breakdown (green), after which the overall MIM resistance was ∼ 200 Ω. The similarity of the two filaments suggests that the physical mechanism leading to "hard" and "soft" breakdown is identical and that only the magnitude of this effect is relevant for the resistive state. Local conductivity investigations on Fe-doped $SrTiO_3$ MIM structures show an increase of conductivity localized to ∼ 1 μm, while the remaining area under the electrode remains highly insulating.[11] The presented μXANES study demonstrates that, during electroforming, the field-induced

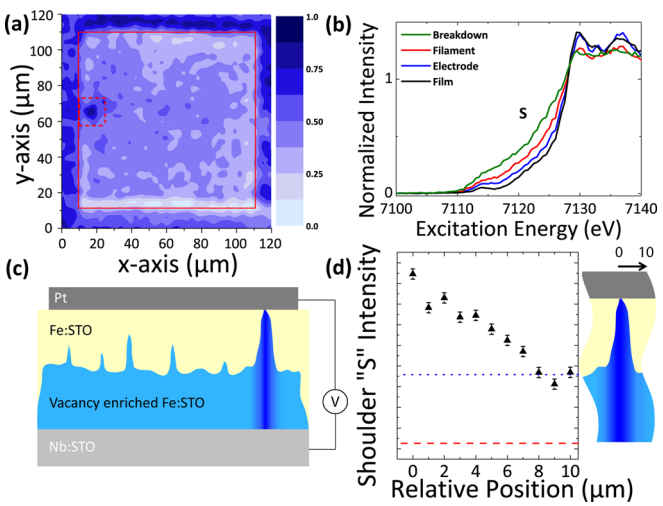


FIG. 3. (a) XY-map of the Fe Kα fluorescence intensity recorded on a $100 \times 100\,\mu m^2$ MIM structure at 7122 eV excitation energy. The solid red line is a guide to the eye, indicating the electrode area. (b) Fe K-edge XANES at the filament (red) and several different (blue) locations on the electrode area, the as-deposited thin film (black), and a different electrode pad after "hard" dielectric breakdown (green). (c) Schematic model of the oxygen vacancy distribution in the switched memristor. (d) Variation of the Fe Kα fluorescence intensity excited at 7122 eV from the center to the border of the conducting filament location.

migration of oxygen vacancies is initially homogeneous over most of the electrode area, until electrical breakdown is achieved at a single point under the electrode. Figure 3(c) combines the conclusions of both experiments in a schematic sketch of the oxygen vacancy distribution in the memristor. The darker color highlights that the filament is structurally different from the surrounding material, as will be discussed later. It is readily apparent from the profile scan shown in Fig. 3(d) that the observed intensity drop is correlated to the beam size on the sample, since the intensity of S has dropped to the level observed on the whole electrode area (indicated by the dotted blue line) when the position of the beam is 7 $\mu$m away from the maximum of S. Since the filament contributes no discernible broadening of the intensity decay, it follows that the diameter is much smaller than the beam size and likely $< 1\,\mu$m. For comparison, the intensity of S observed on the as-deposited film is marked by the dashed red line.

Close examination shows that the Fe K-edge XANES measured at the filament location deviates significantly from that of the surrounding electrode area, with a much stronger increase in intensity of the shoulder S and a decrease of the white line intensity at 7130 eV (Fig. 3(b)). While the homogeneous reduction of the electrode can be interpreted as a simple increase of the Fe-$V_O^{\bullet\bullet}$-concentration, the spectral changes at the location of the filament are further examined through self-consistent, real-space full-multiple-scattering (FMS) XANES calculations[9] by the FDMNES code,[12] performed within the quadrupole and non-muffin-tin approximation using the finite difference method (FDM). Figure 4 elucidates the influence of oxygen vacancies on the shape of the Fe K-edge XANES, demonstrating that the decrease of the white line intensity (peak E) and an increase of the shoulder S intensity (corresponding to the peaks C and D in the calculated XANES), as observed at the location of the filament, can be explained by the presence of an additional oxygen vacancy in the first coordination shell of the Fe atoms. Moreover, a comparison of our XANES calculations with the experiment suggests that the two oxygen vacancies will most likely occupy nearest sites, forming a 90° $V_O^{\bullet\bullet}$-Fe-$V_O^{\bullet\bullet}$ configuration. It is important to note that the FMS simulations are very sensitive to the coordination geometry of Fe, but do not yield any information about the valence state. In the case of a $V_O^{\bullet\bullet}$-Fe-$V_O^{\bullet\bullet}$ complex, the presence of $Fe^{2+}$ cannot be excluded.

In summary, we have shown PLD-grown $SrTi_{0.95}Fe_{0.05}O_3$ thin films to contain $Fe^{3+}$ and a high degree of $Fe^{3+}$-$V_O^{\bullet\bullet}$ associates in the as-deposited state. We demonstrate through micro-focused XANES on a resistively switched MIM structure that electroforming increases the

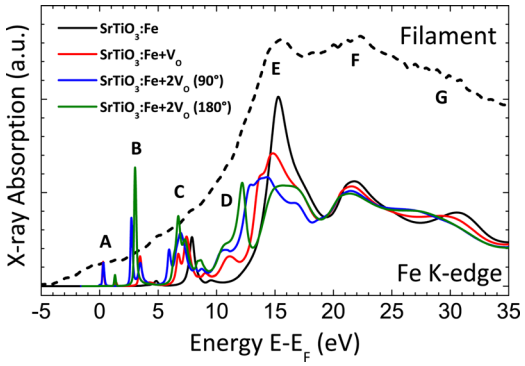


FIG. 4. FMS XANES calculations of the Fe K-edge XANES for undistorted $SrTiO_3$ (black), one vacancy (red), and two vacancies (in 90° (blue) and 180° (green) $V_O^{\bullet\bullet}$-Fe-$V_O^{\bullet\bullet}$ configurations) in the first shell.

Fe-$V_O^{\bullet\bullet}$ concentration homogeneously over the whole electrode area until local breakdown is achieved. FMS XANES calculations suggest that the observed XANES in the region of the conducting filament can be interpreted by the association of two oxygen vacancies to Fe in the filament region.

The authors gratefully acknowledge financial support from the EC FP7 MATERA project FMRSM, the NRW-EU Ziel 2-Programm, and thank ESRF and ID03 beamline personnel (project MA-1082). A.K. and J.P. were supported by the ESF and ERAF Projects 2009/0202/1DP/1.1.1.2.0/09/APIA/VIAA/141 and 2010/0272/2DP/2.1.1.1.0/10/APIA/VIAA/088, respectively.

[1]R. Waser, R. Dittmann, G. Staikov, and K. Szot, Adv. Mater. **21**, 2632 (2009).
[2]R. Waser and M. Aono, Nature Mater. **6**, 833 (2007).
[3]J. P. Strachan, D. B. Strukov, J. Borghetti, J. J. Yang, G. Medeiros-Ribeiro, and R. S. Williams, Nanotechnology **22**, 254015 (2011).
[4]K. Szot, M. Rogala, W. Speier, Z. Klusek, A. Besmehn, and R. Waser, Nanotechnology **22**, 254001 (2011).
[5]J. P. Strachan, G. Medeiros-Ribeiro, J. J. Yang, M.-X. Zhang, F. Miao, I. Goldfarb, M. Holt, V. Rose, and R. S. Williams, Appl. Phys. Lett. **98**, 242114 (2011).
[6]T. Menke, R. Dittmann, P. Meuffels, K. Szot, and R. Waser, J. Appl. Phys. **106**, 114507 (2009).
[7]F. Miao, J. P. Strachan, J. J. Yang, M.-X. Zhang, I. Goldfarb, A. C. Torrezan, P. Eschbach, R. D. Kelly, G. Medeiros-Ribeiro, and R. S. Williams, Adv. Mater. **23**, 5633 (2011).
[8]M. Janousch, G. I. Meijer, U. Staub, B. Delley, S. F. Karg, and B. P. Andreasson, Adv. Mater. **19**, 2232 (2007).
[9]C. Lenser, A. Kalinko, A. Kuzmin, D. Berzins, J. Purans, K. Szot, R. Waser, and R. Dittmann, Phys. Chem. Chem. Phys. **13**, 20779 (2011).
[10]G. I. Meijer, U. Staub, M. Janousch, S. L. Johnson, B. Delley, and T. Neisius, Phys. Rev. B **72**, 155102 (2005).
[11]R. Muenstermann, T. Menke, R. Dittmann, and R. Waser, Adv. Mater. **22**, 4819 (2010).
[12]Y. Joly, Phys. Rev. B **63**, 125120 (2001).